Organic Electronics 13 (2012) 1121–1128

Contents lists available at SciVerse ScienceDirect

Organic Electronics

journal homepage: www.elsevier.com/locate/orgel

Letter

Organic semiconductor heterojunction as charge generation layer in tandem organic light-emitting diodes for high power efficiency

Yonghua Chen [a,1], Qi Wang [b,1], Jiangshan Chen [a], Dongge Ma [a,*], Donghang Yan [a], Lixiang Wang [a]

[a] State Key Laboratory of Polymer Physics and Chemistry, Changchun Institute of Applied Chemistry, Graduate School of the Chinese Academy of Sciences, Chinese Academy of Sciences, Changchun 130022, People's Republic of China
[b] Department of Chemistry, University of North Texas, Denton, TX 76203, USA

ARTICLE INFO

Article history:
Received 12 May 2011
Received in revised form 8 December 2011
Accepted 19 March 2012
Available online 7 April 2012

Keywords:
Tandem organic light-emitting diodes
Organic semiconductor heterojunction
Charge generation layers
Power efficiency

ABSTRACT

High-performance tandem organic light-emitting diodes (OLEDs) employing a buffer-modified C_{60}/pentacene organic semiconductor heterojunction (OHJ) as a charge generation layer (CGL) are demonstrated. The unique cooperation of charge generation, transport, and extraction processes occurred in the OHJ-based CGL remarkably reduces the operational voltage. As a result, an approximately twofold enhancement in power efficiency (21.9 lm W^{-1} VS 10.1 lm W^{-1}) can be achieved that has previously been suggested to be difficult for tandem OLEDs. When the pentacene is replaced by zinc phthalocyanine (ZnPc), copper phthalocyanine (CuPc), or phthalocyanine (H_2Pc), a similar power efficiency improvement can be also achieved. The novel design concept of the buffer-modified OHJ-based CGL is superior to that of the conventional CGLs. The investigations on the operational mechanism are performed, from which it is found that the mobile charge carriers firstly are needed to be accumulated at both sides of the heterojunction interface and then transport along the two organic semiconductors in terms of their good carrier transport characteristics under an external electrical field, and finally inject into the corresponding electroluminescent (EL) units by the interfacial layers.

1. Introduction

Organic light-emitting diodes (OLEDs) can convert injected charges into photons [1]. A single-unit OLED has an upper limit that every injected electron can be converted into at most one photon. Alternatively, a tandem OLED [2–12] that vertically stacks a number of single-unit OLEDs via charge generation layers (CGLs) can convert one injected electron into multiple photons, thus achieving more brightness and current efficiency with lower current density. The CGL, obviously, plays a critical role in the realization of high-performance tandem OLEDs since it functions as both an internal anode and cathode to generate intrinsic charge carriers and to facilitate opposite electron and hole injection into the adjacent sub-OLEDs. Many studies have been conducted to improve the performance of CGLs, most of which have been focused on the development of the *n*-doped/*p*-doped organic junction and *n*-doped organic/transition metal oxide junction for both optimum optical characteristics and electrical properties because they allow for the realization of very efficient tandem devices [2–6,9–12]. However, problems remain. First, the sophisticated and high-cost doping (Li or Cs dopant) process is always required to increase the conductivity of the *n*-type layer in a CGL. In this case, direct contact between this layer and the emissive layer should be avoided to prevent exciton quenching by the highly active alkaline-metal dopants [13]. Furthermore, it is well known that power efficiency (PE) is one key to the commercial realization of a lighting source. However, since

* Corresponding author. Tel.: +86 431 85262357; fax: +86 431 85262873.
E-mail address: mdg1014@ciac.jl.cn (D. Ma).
[1] These authors contributed equally to this work.

1566-1199/$ - see front matter © 2012 Elsevier B.V. All rights reserved.
http://dx.doi.org/10.1016/j.orgel.2012.03.013

the driven voltage consumed by conventional tandem OLEDs scales in a linear fashion with the number of electroluminescent (EL) units, the resulting power consumption to obtain the same luminescence would be the same for both the single-unit and tandem OLEDs, which means that the power efficiency cannot be greatly increased for such tandem devices. Though several factors, including a reduced quenching effect from electrodes, an improved charge recombination balance, and a reduced charge-exciton quenching effect, may contribute to the increase in PE [7], tandem OLEDs still cannot give a satisfactory performance in PE enhancement because they require a high driving voltage. In reality, a large PE improvement in tandem devices can be achieved only if the CGL has excellent charge generation, transport, and carrier injection/extraction capabilities, which allow for a negligible voltage drop across the CGL. Though various CGL structures have been proposed to rectify this issue [3,4,7,14], the PE enhancement is still very limited for presented tandem devices, e.g., Tang and co-workers reported 30–40% enhancement, Forrest and co-workers reported 10–15% enhancement in the high current density, Liao et al. reported 40–50% enhancement, Ryu et al. reported 20–30% enhancement.

Herein, we suggest a novel concept to overcome this problem by using buffer-modified C_{60}/pentacene intrinsic organic semiconductor heterojunction (OHJ) as a CGL in tandem OLEDs. Taking advantage of the charge redistribution occurred at the heterojunction interface, resulting in the fast charge transport and the effective charge extraction, the voltage drop across the CGL is decreased. As a final result, an approximately twofold enhancement in PE (21.9 lm W^{-1} VS 10.1 lm W^{-1}) in tandem OLEDs can be achieved. More importantly, as using zinc phthalocyanine (ZnPc), copper phthalocyanine (CuPc), or phthalocyanine (H_2Pc) to replace pentacene in OHJ as CGL, a similar PE improvement is also obtained, indicating the universality of OHJ as CGL for high-performance tandem OLEDs.

2. Experimental

2.1. Materials

The *n*-type organic semiconductor C_{60} and the *p*-type organic semiconductors pentacene, zinc phthalocyanine (ZnPc), copper phthalocyanine (CuPc), and phthalocyanine (H_2Pc) were purchased from Tokyo Chemical Industry, and the samples were purified twice by thermal gradient sublimation prior to processing. The 4,4′-*N*,*N*′-bis[*N*-(1-naphthyl)-*N*-phenylamino]biphenyl (NPB), 10-(2-Benzothiazolyl)-2,3,6,7-tetrahydro-1,1,7,7-tetramethyl-1*H*,5*H*,11*H*-(1)-benzopyropyran o(6,7-8-*i*,*j*)quinolizin-11-one (C545T), and *tris* (8-hydro xyquinoline) aluminum (Alq_3) were purchased from Nichem Fine Technology Co. Ltd. The MoO_3 were obtained from Alfa Aesar. These materials were used as received.

2.2. Device fabrication

Devices were grown on cleaned glass substrates precoated with a 180 nm thick layer of ITO with a sheet resistance of 10 Ω per square. The ITO surface was treated by oxygen plasma for 2 min, following a decrease in an ultrasonic solvent bath, then it was dried at 120 °C before it was loaded into an evaporator. All layers were deposited by thermal evaporation in succession without breaking the vacuum ($\sim 5 \times 10^{-4}$ Pa). The *n*-type organic semiconductor and *p*-type organic semiconductor used here were evaporated at the rate in a range of 0.1–0.2 nm/s. The other organics and metal oxide were evaporated at the rate in a range of 0.2–0.3 nm/s, and the metals were evaporated at the rate of 0.8–1 nm/s. The doping concentration of C545T in Alq_3 was about 1.0% by volume.

2.3. Measurements

Current-voltage-brightness characteristics were recorded using a computer-controlled sourcemeter (Keithley 2400) and a multimeter (Keithley 2000) with a calibrated silicon photodiode. Capacitance-voltage characteristics were measured with a Keithley 595 quasistatic *CV* meter. Film thickness was monitored by frequency counters and calibrated by a Dektak 6 M profiler (Veeco). The overlap between the ITO and Al electrodes constituted the active emissive area for all devices. The size was 4 mm × 4 mm. All the measurements were carried out in ambient atmosphere at room temperature.

3. Results and discussion

Fig. 1 depicts the schematic diagrams of the corresponding single-unit and tandem OLEDs. The hole and electron transport layers are NPB and Alq_3, respectively. The emissive layer is Alq_3:C545T. In the OHJ CGL, the *n*-type layer is C_{60}, and the *p*-type layer is either pentacene, ZnPc, CuPc, or H_2Pc. The electron and hole extraction layers are LiF and MoO_3, respectively. The general structures of single-unit and tandem OLEDs are ITO/MoO_3(6 nm)/NPB(90 nm)/Alq_3:C545T(30 nm)/Alq_3(30 nm) /LiF (1 nm)/Al(120 nm) and ITO/MoO_3(6 nm)/NPB(90 nm)/Alq_3 : C545T(30 nm)/Alq_3(30 nm)/LiF(0.3 nm)/*n*-type layer (20 nm)/*p*-type layer (15 nm)/MoO_3(3 nm)/NPB(50 nm)/Alq_3 :C545T (30 nm)/Alq_3(30 nm)/LiF(1 nm)/Al(120 nm), respectively. It is noted that the single-unit device shown here is under its optimum structure.

We use C_{60}/pentacene as an example to elucidate our concept. Fig. 2 compares the EL characteristics of the C_{60}/pentacene-based tandem OLED and its single-unit control OLED. Different from the conventional tandem OLEDs [2–12], even though the operational voltage of our tandem device is higher than that of the single-unit device (Fig. 2a), the operational voltage ratio of our tandem device to the single-unit device is gradually decreased with increasing current densities and brightness. For example, at a brightness of 1000 cd m^{-2}, the operational voltage of the tandem device is 10.1 V, whereas that of the single-unit device is 7.2 V. As shown in Fig. 2b, besides that the current efficiency is greatly enhanced from 38 cd A^{-1} of tandem OLEDs to 15.2 cd A^{-1} of single-unit device, the PE of tandem OLED is significantly improved, e.g., $tandem_{max}$: 21.9 lm W^{-1} VS $single\text{-}unit_{max}$: 10.1 lm W^{-1} (Fig. 2c), which beyond doubt gives the best PE improvement reported so far for tandem devices without any out-coupling

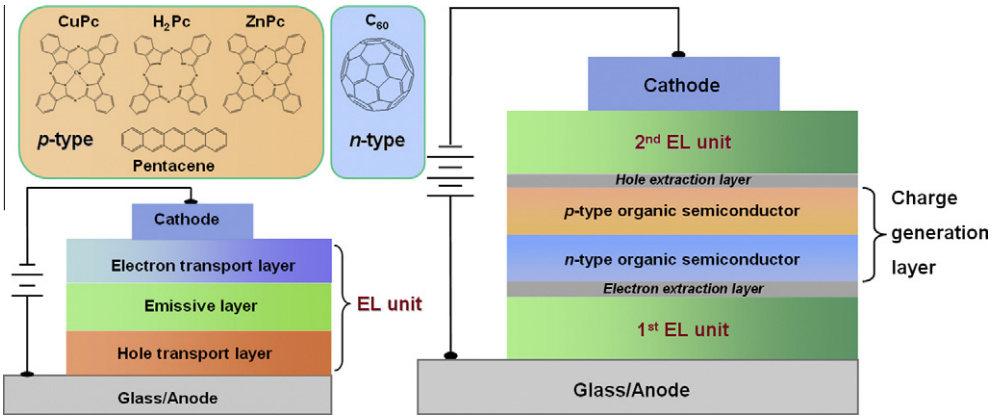

Fig. 1. Schematic diagram of the single-unit (left) and tandem (right) devices. The molecular structures of C_{60}, pentacene, ZnPc, CuPc, and H_2Pc are shown at the top-left.

technique [15–17]. Even at high brightness the PE enhancement is still significant, for example, under 1000, 10,000, and 38,000 cd m^{-2}, the PE enhancements come to 1.74, 1.81 and 1.9 times over that of the optimized single-unit, respectively, making this CGL much superior to the conventional ones [3,4,7]. Furthermore, when the pentacene is replaced by H_2Pc, ZnPc or CuPc, a similar PE improvement can be also achieved. As shown in Fig. 3, the reduced operational voltage (Fig. 3a) and the double current efficiency (Fig. 3b) are also obtained in C_{60}/ZnPc, C_{60}/CuPc, and C_{60}/H_2Pc-based tandem OLEDs compared to that of the single-unit OLED. Importantly, the maximum power efficiency of 21, 18.6 and 16.1 lm W^{-1} can also be achieved, indicating that the OHJ-based CGL is a universal concept for high-performance tandem OLEDs. Table 1 summarizes the device performances of all tandem and single-unit OLEDs.

To clarify the PE improvement in the buffer-modified C_{60}/pentacene-based tandem device, a profound understanding of the charge generation and extraction that occur in the CGL is required. First, direct experimental evidence is provided by investigating the capacitance-voltage (*C*–*V*) characteristics of the intentionally-designed devices. The device structures are ITO/LiF(100 nm)/Alq_3(30 nm)/NPB(50 nm)/LiF(100 nm)/Al(120 nm) (device 1), ITO/LiF (100 nm)/Alq_3(30 nm)/C_{60}(20 nm)/pentacene(15 nm)/NPB (50 nm)/LiF(100 nm)/Al(120 nm) (device 2), and ITO/LiF (100 nm)/Alq_3(30 nm)/LiF(0.3 nm)/C_{60}(20 nm)/pentacene (15 nm)/MoO_3(3 nm)/NPB(50 nm)/LiF(100 nm)/Al(120 nm) (device 3), respectively. We note that 100 nm-thick LiF layers serve as insulating layers to block the charge injection from the outside electrodes in all devices. As shown in Fig. 4, it can be seen that device 1 exhibits no change in capacitance with the applied voltages from −20 to 20 V. This constant capacitance indicates that the LiF film indeed acted as an insulator layer and completely blocked charge injection from the external electrodes ITO and Al in this voltage range. Furthermore, it also indicates that neither the displacement nor the generation of charges within NPB and Alq_3 layers occurs. Compared to the non-CGL-equipped device 1, device 2 exhibits a gradual increase of capacitance over 5 V. We attribute this increased capacitance in the positive voltage to the larger dielectric constants of the C_{60}/pentacene bilayers (devices 2 and 3) coming from the larger polarization of the charge transfer complexes from pentacene to C_{60} due to the exceptionally strong acceptor character of C_{60} molecules and the close energy levels of C_{60} and pentacene. This fact conclusively proves that an electric-field-induced charge generation process takes place at the C_{60}/pentacene interface. In the negative voltage, however, there should only be charge recombination not generation at the C_{60}/pentacene interface. The higher capacitance in devices 2 and 3 compared to device 1 can be attributed to the interfacial dipole, which also leads to larger polarization in C_{60}/pentacene interface. We will discuss below in detail.

Charge generation is a prerequisite to the CGL operation. The generated charge carriers have to be extracted out of the CGL and then injected into the adjacent sub-OLEDs. Previous reports emphasized the generation process [8], however, herein we note that an effective charge extraction is also essential, in particular for the PE improvement. In fact, the large injection barriers remain between C_{60} and Alq_3 and between pentacene and NPB (LUMOs: 3.0 eV for Alq_3 and 4.5 eV for C_{60}, HOMOs: 5.5 eV for NPB and 4.9 eV for pentacene) [18,19]. In our tandem device (Fig. 1), LiF and MoO_3 buffers are introduced to modify C_{60} and pentacene, respectively. This is strikingly different from the previous report by Rao et al. where only 34% improvement in current efficiency (2.5–3.4 cd A^{-1}) is achieved compared to the corresponding single-unit device at a current density of 20 mA cm^{-2} [20], whereas the current efficiency can remarkably be improved by 2.5 times (14.9–37.8 cd A^{-1}) in our tandem device. It can be seen from the *C*–*V* characteristics that with the increase of voltages, large amount of charge carriers can be generated at the interface of C_{60}/pentacene and the generated charge carriers can be significantly increased. Therefore, the significant enhancement in current efficiency can be attributed to the better charge balance between the generated carriers from the CGL and the injected carriers from the external electrodes due to the

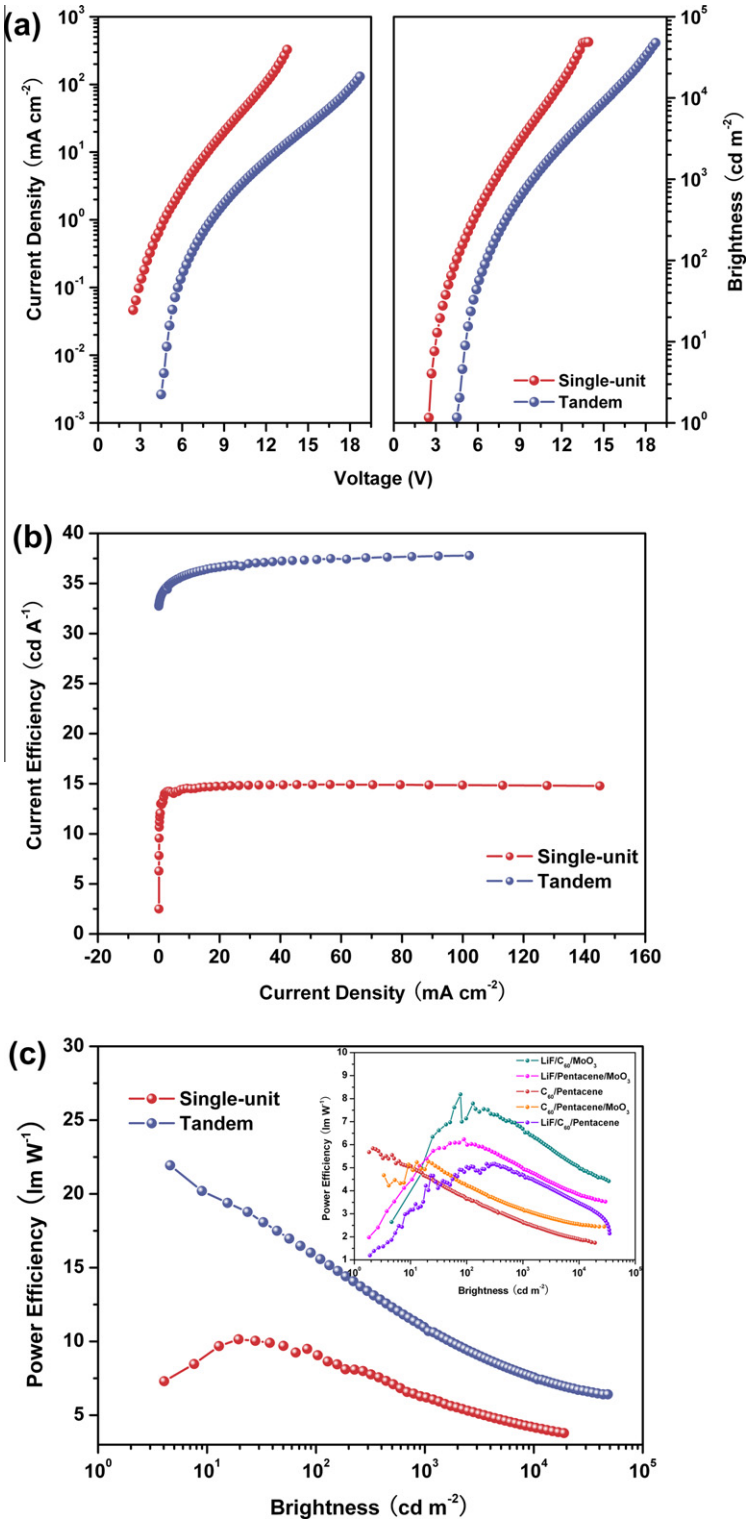

Fig. 2. EL performances of the single-unit and tandem OLEDs. (a) The current density-voltage-brightness characteristics. (b) The current efficiency and (c) the power efficiencies of the single-unit and LiF/C_{60}/pentacene/MoO_3-based tandem OLEDs. Inset: the power efficiencies of the control tandem devices, in which the CGLs are assembled with different material combinations.

generation of large amount of charge carriers in CGL, especially in the high voltage, and the effectively injection of the generated charge carriers into corresponding EL units. As we see, without either buffer modified layers, the PE

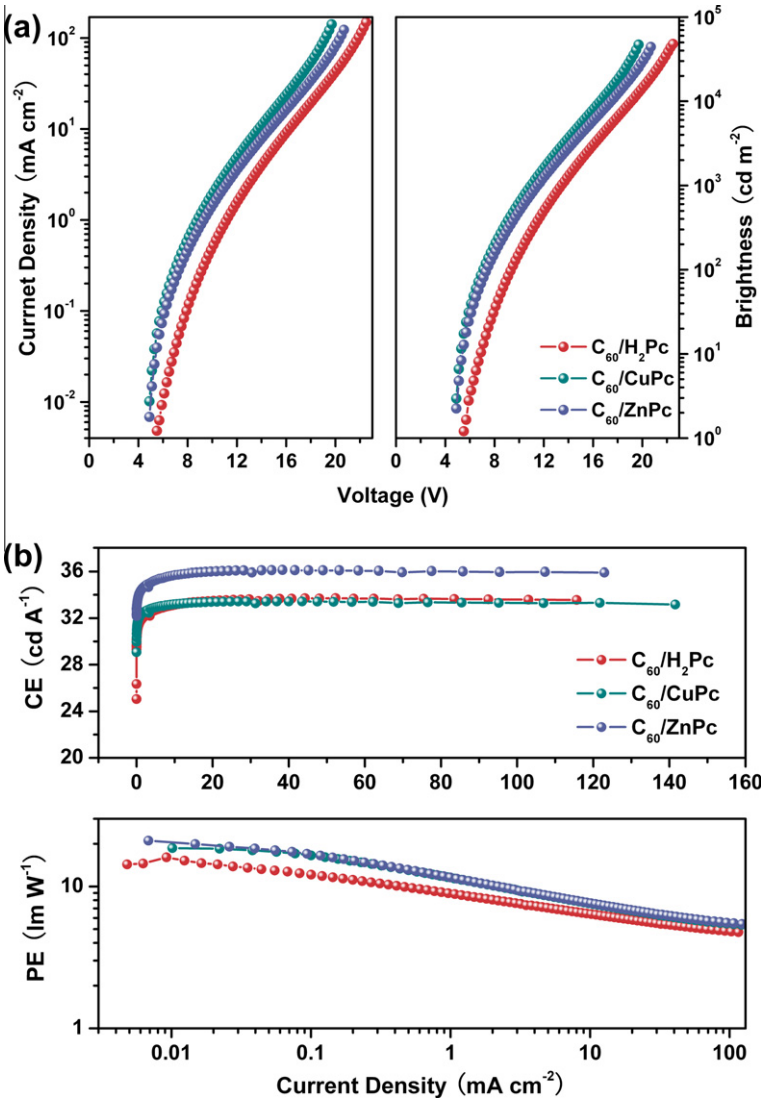

Fig. 3. EL performances of tandem OLEDs based on buffer-modified C_{60}/ZnPc, C_{60}/CuPc or C_{60}/H_2Pc as CGLs. (a) The current density-voltage-brightness characteristics. (b) The power efficiency (PE) and current efficiency (CE) characteristics as a function of current density.

Table 1
Summary of device characteristics by exploiting single-unit and tandem architectures.

CGL	V_t[a] [V]	B[b] [cd m^{-2}]	$\eta_{CE,\ max}$[c] [cd m^{-2}]	η_{CE}[b] [cd A^{-1}]	$\eta_{PE,max}$[d] [lm W^{-1}]	η_{PE}[b] [lm W^{-1}]
No[e]	2.5	3033	14.9	14.8	10.1	5.1
LiF/C_{60}/pentacene/MoO_3	4.9	7322	37.8	36.6	21.9	7.9
LiF/C_{60}/ZnPc/MoO_3	4.9	7022	36.1	35.8	21	6.8
LiF/C_{60}/CuPc/MoO_3	5.1	6547	33.4	33.4	18.6	6.7
LiF/C_{60}/H_2Pc/MoO_3	5.3	6527	33.5	33.5	16	5.8
BCP:Li/MoO_3	5.5	6131	31.7	30.7	11.6	4.7
BCP:Li/NPB:MoO_3	5.5	5998	31	30.4	11.3	4.7

[a] V_t: Turn-on voltage examined at the brightness of 1 cd m^{-2}.
[b] B: Brightness. η_{CE}:current efficiency, and η_{PE}: power efficiency obtained at the current density of 20 mA cm^{-2}.
[c] $\eta_{CE,\ max}$: maximum value of current efficiency.
[d] $\eta_{PE,max}$: maximum value of power efficiency.
[e] Single-unit device.

of the resulting device is even worse than that of the single-unit device (Fig. 2c and its inset), indicating the formation of energy barriers that are unfavorable to the charge injection into the adjacent EL units. Accordingly,

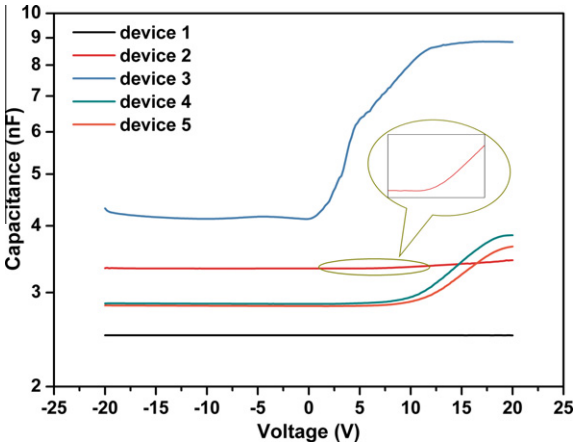

Fig. 4. *C–V* characteristics of five devices measured at a fixed frequency of 1000 Hz.

higher driving voltages are required to drive the charges across the energy barriers, leading to a PE reduction. The *C–V* examinations are used here to support this point. Compared to the non-buffer-modified device 2, the threshold voltage for the capacitance increase in device 3, which equips buffers on both sides of C_{60}/pentacene heterojunction, diminishes from 5 to 0 V, and the magnitude of the capacitance increase is much larger in device 3 (Fig. 4). Actually, LiF [21–23] and MoO_3 [18,24] are very good electron and hole interfacial injection materials and widely used in OLEDs to reduce electron and hole injection barriers. Our results also clearly indicate the important role of the introduced buffer-modified layers LiF and MoO_3 in OHJ CGL in reducing the electron and hole injection barriers into corresponding EL units, thus reducing operational voltage and improving PE.

To further demonstrate the merit of this novel CGL, we fabricated another two control tandem OLEDs by using the well-investigated *n*-doped organic/transition metal oxide junction 2,9-dimethyl-4,7-diphenyl-1,10-phenanthroline (BCP): Li/MoO_3 and the *n*-doped/*p*-doped organic junction BCP: Li/4,4′-*N*,*N*′-bis[*N*-(1-nap-hthyl)-*N*-phenyl-amino]biphe nyl (NPB): MoO_3 as CGLs [3,9,11,25]. As shown in Fig. 5, both of the optimized devices achieved a twofold enhancement in current efficiency (Table 1 and Fig. 5a, 31.7 and 31 cd A^{-1} for BCP:Li/MoO_3 and BCP:Li/NPB:MoO_3, respectively) but barely showed an improvement in PE as compared to the single-unit counterpart (Table 1 and Fig. 5b, 11.6 and 11.3 lm W^{-1} for BCP:Li/MoO_3 and BCP:Li/NPB:MoO_3, respectively). This fact indicates that the buffer-modified OHJ CGL is superior to the conventional CGLs. The *C–V* examinations confirm why the buffer-modified C_{60}/pentacene CGL is superior to both the traditional *n*-doped organic/transition metal oxide and the *n*-doped/*p*-doped organic junction CGLs. The device structures for capacitance measurement are ITO/LiF(100 nm)/Alq_3(30 nm)/BCP: Li(20 nm)/MoO_3(3 nm)/NPB(50 nm)/LiF (100 nm)/Al(120 nm) (device 4) and ITO/LiF(100 nm)/Alq_3(30 nm)/BCP: Li(20 nm)/NPB: MoO_3(40 nm)/NPB(50 nm)/LiF(100 nm)/Al(120 nm) (device 5). As shown in Fig. 4, the threshold voltage for the capacitance increase in device 4 (based on BCP: Li/MoO_3) and 5 (based on BCP: Li/NPB: MoO_3) is 3 V over that of device 3 (based on LiF/C_{60}/pentacene/MoO_3),

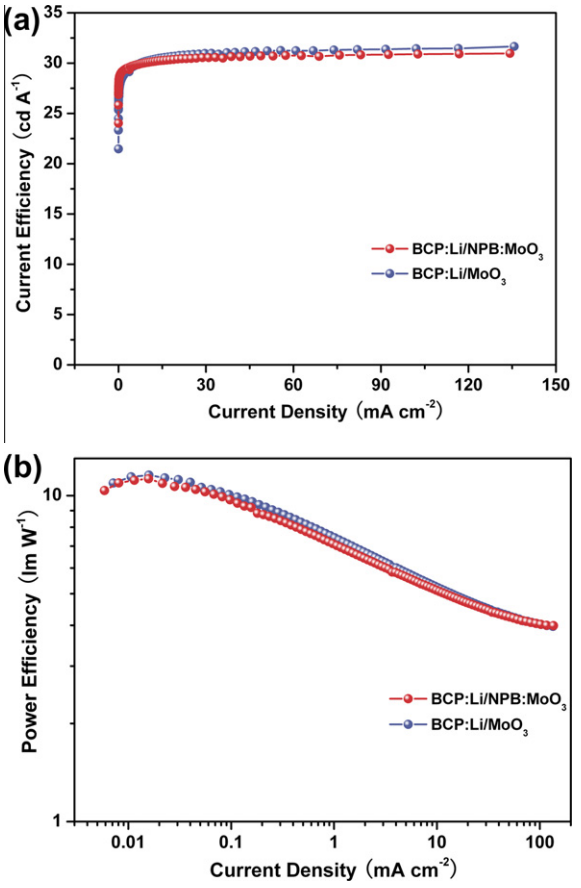

Fig. 5. EL performances of tandem OLEDs based on BCP: Li/MoO_3 BCP: Li/NPB: MoO_3 as CGLs. (a) The current efficiency characteristics as a function of current density. (b) The power efficiency characteristics as a function of current density.

while the capacitance values of device 4 and 5 are less than 50% that of device 3 under the same bias. This fact irrefutably demonstrates that our CGL is able to generate more charge carriers than conventional CGLs, allowing for a reduction of driven voltage and thus the twofold enhancement in PE in tandem devices.

Apparently, the significant PE improvement in our tandem devices comes from the efficient charge generation and extraction that occur in the buffer-modified OHJ CGL. Various concepts have been proposed to elucidate the mechanism of charge generation, including temperature-independent, field-induced charge separation for doped organic *p–n* heterojunction CGLs, [11] interfacial electron transfer from *p*-type layer to metal oxide due to the interfacial dipole-induced energy level alignment for transition metal oxide-based CGLs [12,26,27], and the energy barrier-induced interfacial charge accumulation for polymer CGL [13]. Before we go any further, we must clarify one fact: the MoO_3/NPB contact, which can provide a matching energy level alignment to allow for an electron redistribution (known as generation) from NPB to MoO_3 [27], is not the origin of PE enhancement in our tandem devices, since removing either C_{60} (CGL:

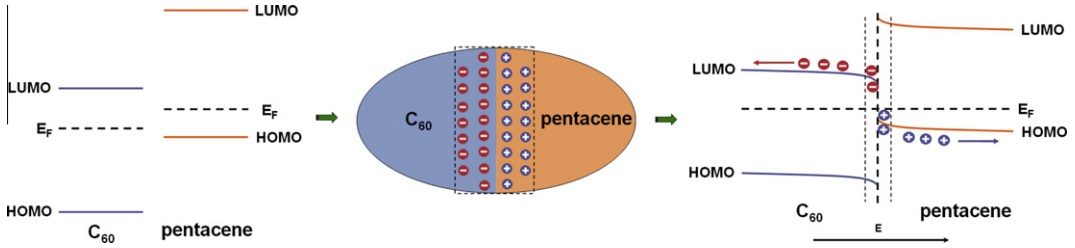

Fig. 6. Proposed working principle of the C_{60}/pentacene heterojunction constructed CGL. E_F: Fermi energy level; LUMO: lowest unoccupied molecular orbital; HOMO: highest occupied molecular orbital.

LiF/pentacene/MoO_3) or pentacene (CGL: LiF/C_{60}/MoO_3) in our CGL will significantly increase the driven voltage and hence decrease the PE (the inset of Fig. 2c). Alternatively, this NPB/MoO_3 interfacial electron-transfer can energetically facilitate the hole injection from MoO_3 to NPB [27], indicating that the MoO_3 here serves as a buffer layer. Hence, the C_{60}/pentacene heterojunction plays a crucial role in our CGL operation.

Several groups have successfully described the electronic structures of the C_{60}/pentacene heterojunction [28–31]. The fact that interfacial dipole is formed at the interface is well established [29,30]. In reality, the interfacial dipole may originate from interfacial charge-transfer, polarization effects induced by an asymmetric electronic density distribution, interfacial chemical reaction, and alignment of charge neutrality levels [27,32–34]. Also recent theoretical simulation shows that the abrupt imbalance in molecular quadrupoles should be the origin of the dipole formation for the case of C_{60}/pentacene heterojunction [29]. In any case, the interfacial dipole formation is beneficial to the energy level alignment of the C_{60}/pentacene interface, thus facilitating the electron-transfer from pentacene to C_{60} that has been observed previously [28,30]. This fact is also supported by the theory of thermal emission of electrons, since pentacene holds a higher Fermi level than C_{60} at flat band (Fig. 6 left). Also noted is that this charge-transfer in turn contributes to the interfacial energy level equilibrium.

Taking great benefit from the charge redistribution, the electrons and holes can be, respectively, accumulated on the *n*-type C_{60} and *p*-type pentacene in the vicinity of the C_{60}/pentacene interface (Fig. 6 middle). Therefore, high-density free electrons and holes are provided at the C_{60}/pentacene junction, which can move away from the interface in opposite directions under an external electric field (Fig. 6 right). This process is beneficial to reducing the voltage drop across the CGL and hence the reduction of the overall driving voltage during the device operation. Analogous conclusions can be applied to explain the PE improvement in the cases of C_{60}/ZnPc, C_{60}/CuPc and C_{60}/H_2Pc junctions because the ground state electron transfer can also efficiently take place from ZnPc, CuPc or H_2Pc to C_{60}, which has been investigated with UV–Vis-NIR absorption spectroscopy and by theoretical calculations [35,36]. Obviously, the relative energy level of both semiconductor components is very important for the CGL construction, which directly determines the charge generation.

4. Conclusions

In summary, a novel design concept, that is, utilizing buffer-modified organic semiconductor heterojunction as a CGL in tandem OLEDs has been proposed, under which an approximately twofold improvement (21.9 VS 10.1 lm W^{-1}) in power efficiency of tandem OLEDs can be realized. The unique working principle of this organic heterojunction constructed CGL makes it superior to other today's state-of-arts CGLs since it allows for an interfacial electron redistribution to supply high-density free charges, efficiently decreasing the voltage drop across it. This new and doping-free heterojunction-type CGL also offer a low-cost fabrication process and a rich choice of materials combination, suggesting its great commercial prospect as compared to the conventional CGLs. We believe that the concept of organic heterojunction opens new perspectives for the rational design of CGL to realize tandem devices with unprecedented improvement in power efficiency, in particular its having great potential in fabricating tandem white OLEDs for solid-state-lighting.

Acknowledgements

The authors thank the Science Fund for Creative Research Groups of NSFC (20921061), the National Natural Science Foundation of China (50973104, 60906020), Ministry of Science and Technology of China (973 program No. 2009CB623604, 2009CB930603), the Foundation of Jilin Research Council (20080337, 20090127) for the support of this research.

References

[1] M. Segal, M. Singh, K. Rivoire, S. Difley, T.V. Voorhis, M.A. Baldo, Nat. Mater. 6 (2007) 374.
[2] T. Matsumoto, T. Nakada, J. Endo, K. Mori, N. Kawamura, A. Yokoi, J. Kido, SID 03 Digest. 34 (2003) 979.
[3] L.S. Liao, K.P. Klubek, C.W. Tang, Appl. Phys. Lett. 84 (2004) 167.
[4] H. Kanno, R.J. Holmes, Y. Sun, S.K. Cohen, S.R. Forrest, Adv. Mater. 18 (2006) 339.
[5] C.C. Chang, J.F. Chen, S.W. Hwang, C.H. Chen, Appl. Phys. Lett. 87 (2005) 253501.
[6] C.W. Chen, Y.J. Lu, C.C. Wu, E.H. Wu, C.W. Chu, Y. Yang, Appl. Phys. Lett. 87 (2005) 241121.
[7] L.S. Liao, K.P. Klubek, Appl. Phys. Lett. 92 (2008) 223311.
[8] S.L. Lai, M.Y. Chan, M.K. Fung, C.S. Lee, S.T. Lee, J. Appl. Phys. 101 (2007) 014509.
[9] T.Y. Cho, C.L. Lin, C.C. Wu, Appl. Phys. Lett. 88 (2006) 111106.
[10] J.X. Sun, X.L. Zhu, H.J. Peng, M. Wong, H.S. Kwok, Org. Electron. 8 (2007) 305.

[11] M. Kröger, S. Hamwi, J. Meyer, T. Dobbertin, T. Riedl, W. Kowalsky, H.H. Johannes, Phys. Rev. B 75 (2007) 235312.
[12] S. Hamwi, J. Meyer, M. Kröger, T. Winkler, M. Witte, T. Riedl, A. Kahn, W. Kowalsky, Adv. Funct. Mater. 20 (2010) 1762.
[13] S.J. Su, T. Chiba, T. Takeda, J. Kido, Adv. Mater. 20 (2008) 2125.
[14] S.Y. Ryu, J.T. Kim, J.H. Noh, B.H. Hwang, C.S. Kim, S.J. Jo, H.S. Hwang, S.J. Kang, H.K. Baik, C.H. Lee, S.Y. Song, S.J. Lee, Appl. Phys. Lett. 92 (2008) 103301.
[15] Y. Sun, S.R. Forrest, Nat. Photonics 2 (2008) 483.
[16] W.H. Koo, S.M. Jeong, F. Araoka, K. Ishikawa, S. Nishimura, T. Toyooka, H. Takezoe, Nat. Photonics 4 (2010) 222.
[17] S. Reineke, F. Lindner, G. Schwartz, N. Seidler, K. Walzer, B. Lussem, K. Leo, Nature 459 (2009) 234.
[18] H. You, Y. Dai, Z. Zhang, D. Ma, J. Appl. Phys. 101 (2007) 026105.
[19] S. Yoo, B. Domercq, B. Kippelen, Appl. Phys. Lett. 85 (2004) 5427.
[20] M.V.M. Rao, T.-S. Huang, Y.-K. Su, Y.-T. Huang, J. Electrochem. Soc. 157 (2010) H69.
[21] L.S. Hung, C.W. Tang, M.G. Mason, Appl. Phys. Lett. 70 (1997) 152.
[22] H. Heil, J. Steiger, S. Karg, M. Gastel, H. Ortner, H. von Seggern, M. Stößel, J. Appl. Phys. 89 (2001) 420.
[23] M.G. Mason, C.W. Tang, L.-S. Hung, P. Raychaudhuri, J. Madathil, D.J. Giesen, L. Yan, Q.T. Le, Y. Gao, S.-T. Lee, L.S. Liao, L.F. Cheng, W.R. Salaneck, D.A. dos Santos, J.L. Brédas, J. Appl. Phys. 89 (2001) 2756.
[24] F. Wang, X. Qiao, T. Xiong, D. Ma, Org. Electron. 9 (2008) 985.
[25] Q. Wang, J. Ding, Z. Zhang, D. Ma, Y. Cheng, L. Wang, F. Wang, J. Appl. Phys. 105 (2009) 076101.
[26] J. Meyer, M. Kröger, S. Hamwi, F. Gnam, T. Riedl, W. Kowalsky, A. Kahn, Appl. Phys. Lett. 96 (2010) 193302.
[27] Q. Bao, J. Yang, Y. Li, J. Tang, Appl. Phys. Lett. 97 (2010) 063303.
[28] S.J. Kang, Y. Yi, C.Y. Kim, K. Cho, J.H. Seo, M. Noh, K. Jeong, K.H. Yoo, C.N. Whang, Appl. Phys. Lett. 87 (2005) 233502.
[29] S. Verlaak, D. Beljonne, D. Cheyns, C. Rolin, M. Linares, F. Castet, J. Cornil, P. Heremans, Adv. Funct. Mater. 19 (2009) 3809.
[30] S.J. Kang, Y. Yi, C.Y. Kim, S.W. Cho, M. Noh, K. Jeong, C.N. Whang, Synth. Met. 156 (2006) 32.
[31] I. Salzmann, S. Duhm, R. Opitz, R.L. Johnson, J.P. Rabe, N. Koch, J. Appl. Phys. 104 (2008) 114518.
[32] H. Ishii, K. Sugiyama, E. Ito, K. Seki, Adv. Mater. 11 (1999) 605.
[33] I. Avilov, V. Geskin, J. Cornil, Adv. Funct. Mater. 19 (2009) 624.
[34] H. Vázquez, W. Gao, F. Flores, A. Kahn, Phys. Rev. B 71 (2005) 041306(R).
[35] K. Akaike, K. Kanai, Y. Ouchi, K. Seki, Adv. Funct. Mater. 20 (2010) 715.
[36] A. Ray, D. Goswami, S. Chattopadhyay, S. Bhattacharya, J. Phys. Chem. A 112 (2008) 11627.